International Journal of Automotive Technology, Vol. 15, No. 6, pp. 989–1000 (2014)
DOI 10.1007/s12239–014–0104–9

pISSN 1229–9138/ eISSN 1976–3832

COOPERATIVE REGENERATIVE BRAKING CONTROL FOR FRONT-WHEEL-DRIVE HYBRID ELECTRIC VEHICLE BASED ON ADAPTIVE REGENERATIVE BRAKE TORQUE OPTIMIZATION USING UNDER-STEER INDEX

J. HAN, Y. PARK* and Y. PARK

Department of Mechanical Engineering, KAIST, Daejeon 305-701, Korea

(Received 29 April 2013; Revised 14 November 2013; Accepted 14 November 2013)

ABSTRACT–In this study, cooperative regenerative braking control of front-wheel-drive hybrid electric vehicle is proposed to recover optimal braking energy while guaranteeing the vehicle lateral stability. In front-wheel-drive hybrid electric vehicle, excessive regenerative braking for recuperation of the maximum braking energy can cause under-steer problem. This is due to the fact that the resultant lateral force on front tire saturates and starts to decrease. Therefore, cost function with constraints is newly defined to determine optimum distribution of brake torques including the regenerative brake torque for improving the braking energy recovery as well as the vehicle lateral stability. This cost function includes trade-off relation of two objectives. The physical meaning of first objective of cost function is to maximize the regenerative brake torque for improving the fuel economy and that of second objective is to increase the mechanical-friction brake torques at rear wheels rather than regenerative brake torque at front wheels for preventing front tire saturation. And weighting factor in cost function is also proposed as a function of under-steer index representing current state of the vehicle lateral motion in order to generalize the constrained optimization problem including both normal and severe cornering situation. For example, as the vehicle approaches its handling limits, adaptation of weighting factor is possible to prioritize front tire saturation over increasing the recuperation of braking energy for driver safety and vehicle lateral stability. Finally, computer simulation of closed loop driver-vehicle system based on Carsim™ performed to verify the effectiveness of adaptation method in proposed controller and the vehicle performance of the proposed controller in comparison with the conventional controller for only considering the vehicle lateral stability. Simulation results indicate that the proposed controller improved the performance of braking energy recovery as well as guaranteed the vehicle lateral stability similar to the conventional controller.

KEY WORDS : Cooperative regenerative braking control, Front-wheel-drive hybrid electric vehicle, Vehicle lateral stability, Adaptive regenerative brake torque optimization

NOMENCLATURE

BCU : Brake Control Unit
MCU : Motor Control Unit
BMU : Battery Manage Unit
VCU : Vehicle Control Unit
m : total mass of the vehicle (kg)
a_x, a_y : longitudinal/lateral acceleration
V_x : longitudinal velocity of a vehicle (m/s)
δ_f : front steering angle (rad)
β_{des}, β : desired and real side-slip angle (rad)
ψ_{des}, ψ : desired and real yaw angle (rad)
Y_F, Y_R : total lateral tire force of the front, rear wheel in bicycle model (N)
X_F, X_R : total longitudinal tire force of the front, rear wheel in bicycle model (N)
X_{FL}, X_{FR} : longitudinal tire force of the front-left, front-right wheel (N)
X_{RL}, X_{RR} : longitudinal tire force of the rear-left, rear-right wheel (N)
$X_{regn.}$: regenerative braking force of the front wheel (N)
X_{des} : desired longitudinal tire force by driver (N)
I_Z : moment of inertia about yaw axis (kgÞm^2)
l_F, l_R : distance from the center of gravity to front axle, to rear axle (m)
t : track width (m)
C_F, C_R : front, rear tire cornering stiffness in bicycle model (N/rad)
α_F, α_R : slip angle of the front, rear tire in bicycle model (rad)
α_{FL}, α_{FR} : slip angle of the front-left, front-right tire (rad)
α_{FL}, α_{RR} : slip angle of the rear-left, rear-right tire (rad)
$M_{control}$: yaw moment by upper-level controller (Nm)
r_{eff} : radius of a wheel (m)
ξ : gear ratio
ω_{des} : desired motor speed (rad/s)

*Corresponding author. e-mail: yjpark@kaist.ac.kr

1. INTRODUCTION

The large number of automobiles around the world caused serious problems for environment and human life such as air pollution, global warming, and the rapid depletion of the Earth's petroleum resources. Electric vehicles (EVs), hybrid electric vehicles (HEVs), and fuel cell hybrid electric vehicles (FCHEVs) have been widely studied in recent years because of its potential to significantly improve fuel economy and reduce emissions of ground vehicles. EVs, HEVs, FCHEVs have one more electric motors to drive the vehicle and to recover the significant amounts of the braking energy. This is one of the most features of EVs, HEVs, and FCHEVs to improve fuel economy because braking energy stored in the energy storage system can be reused. Because of the limited regenerative braking by motor specification, almost EVs, HEVs, and FCHEVs additionally have mechanical-friction brake system for vehicle stability.

In the hybrid braking system which coexists with regenerative braking and mechanical-friction braking, several control strategies have been studied for ensuring the vehicle braking performance in longitudinal direction and its ability to recover as much braking energy as possible for EVs or HEVs. Mutoh considered EV with a structure that can drive the front and rear wheels independently. The method using estimated vehicle speed, acceleration, and load movement distributes the braking torque to the front and rear wheels according to longitudinal driving condition in order to prevent wheel lock and slip phenomena and to improve the riding comfort (Mutoh *et al*., 2007). Gao investigated the braking energy characteristics on vehicle speed and braking power in typical urban driving cycles. And two hybrid braking systems which are parallel hybrid braking system and fully controllable hybrid system for EVs, HEVs, and FCVs are proposed to consider optimal braking performance and optimal braking energy recovery in longitudinal direction (Gao *et al*., 2007). Chu proposed integrative braking control strategy for recovering the braking energy as well as maintaining a good braking performance for vehicle safety in longitudinal direction. The braking force distribution theory and the stipulated Economic Commission for Europe (ECE) regulation are used to design an integrative braking control strategy (Chu *et al*., 2009). Hellgren investigated the relation between the regenerative braking energy and the related properties, and presented a computational procedure using genetic algorithm to maximize the regenerative braking energy according to specific drive cycle in longitudinal direction (Hellgren and Jonasson, 2007). Oleksowicz also investigated the relation between anti-lock braking system and regenerative braking (Oleksowicz *et al*., 2013). Jingming proposed parallel regenerative brake strategy for the brake safety and the largest amount of the brake energy. This proposed strategy is optimized on Saturn SL1 (Jingming *et al*., 2008).

A few studies in the literatures can be found, which maintain the vehicle lateral stability enhancement using motor. Advanced motion controls for 4 wheel-motored EV are proposed to improve the vehicle lateral stability by using regenerative braking from each of the 4 motors, even in the non-linear region of tire (Hori, 2004; Sakai *et al*., 1999; Shino and Nagai, 2003). Kim considered 4-wheel-drive HEV which has the regenerative brake torque of rear motor and electro-hydraulic brake (EHB) torques with optimal distribution ratio. A fuzzy-rule-based control is chosen to determine the direct yaw moment. In order to improve the vehicle lateral stability, regenerative brake torque at rear wheel generates yaw moment first, and then EHB with the optimal distribution ratio works to compensate for insufficient yaw moment. This optimal distribution ratio of the EHB is presented to minimize the EHB power consumption (Kim and Kim, 2006). Kim also used genetic algorithm to obtain the optimal torque distribution between the regenerative brake torque from rear motor and the EHB torques. Optimization process is repeated for various road and desired yaw moment in order to obtain optimal regenerative brake torque at rear wheel and EHB torque at front and rear wheel (Kim *et al*., 2007). Hancock investigated the impact on the vehicle lateral stability of applying regenerative braking through the rear axle. In order to guarantee the vehicle lateral stability, two strategies are proposed; first one is switching to friction braking with fixed ratio when slip of rear wheel exceeds a specified threshold, and second on is locking the centre coupling, which allows to distribute regenerative braking to front and rear axles (Hancock and Assadian, 2006).

This paper considers only front-wheel-drive hybrid electric vehicle, as shown in figure 1. In front-wheel-drive hybrid electric vehicle, an electric motor for regenerative braking is only connected to the front axle, and mechanical-friction braking such as EMB (Electro-Mechanical Brake), EWB (Electro-Wedge Brake) can be independently applied on each of the 4 wheels. During every day driving situations, normal drivers usually brake the vehicle well within the physical limit of adhesion of the tires. However, as the vehicle approaches its handling limits, for example during an evasive double lane change or constant turning on the slippery road, the vehicle tends to respond less predictably to the driver's steer input. Especially, if

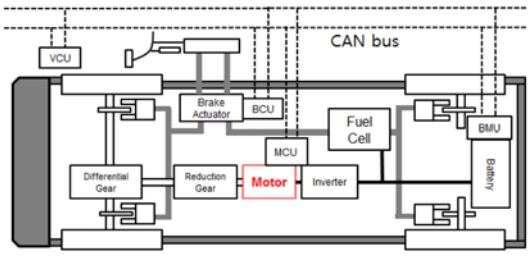

Figure 1. System configuration of the front-wheel-hybrid electric vehicle.

excessive regenerative brake torque is applied at front wheels, the vehicle can lose the vehicle lateral stability such as under-steer problem, i.e., the vehicle may plow out of the desired path. This instability will cause large steer angle for driver to track the desired path and even loss of control. This is due to the fact that electric motor can be employed to only brake the front wheels for regenerative braking.

Therefore, cooperative regenerative braking control strategy is proposed to enhance braking energy recovery while guaranteeing the vehicle lateral stability. Constrained optimization with cost function and constraint is formulated in order to obtain an optimal regenerative braking torque. The cost function is defined as weighted sum of both maximizing the recuperation of braking energy and the decreasing the regenerative braking for preventing front tire saturation. When the vehicle comes to limited adhesion of tire, the lateral force is saturated and starts to be decreased by braking force. Fiction circle concept is used to estimate the change of resultant lateral force by braking force, and the value of estimation is included the yaw moment constraint (Han *et al*., 2011). Simulation results showed that cost function with constraint which includes the estimation of lateral force variation can stabilize the vehicle lateral motion as well as enhancement of braking energy recovery in severe cornering. In other way, cost function is more weighted front tire saturation than the recuperation of braking energy for driver safety and vehicle lateral stability. In severe cornering, another weighting factor which is appropriate for severe cornering situation can make improve the vehicle lateral stability performance compared with weighting factor of normal cornering (Han *et al*., 2011). In this study, to generalize the constrained optimization problem including both normal and severe cornering situations, adaptation method of weighting factor is proposed. Therefore, weighting factor is defined as function of under-steer index which represents the current state of the vehicle lateral motion. Weighting factor is possible to prevent the loss of control for the vehicle even in severe cornering condition and to improve the fuel economy in normal cornering condition because that it can be automatically varied in real-time according to the vehicle lateral motion. Driving mode easily affects the vehicle lateral stability (Wang *et al*., 2013), thus, we describe some simulated environments such as severe cornering situation, normal braking scenario on slippery road, etc. And then, by using CarSim™ software, several simulations were performed to verify the effectiveness of the adaptation method and compare its vehicle performance with conventional controller.

The following descriptions are the section outlines of this paper. In section 2, the design procedure of the cooperative regenerative braking controller for satisfying 2 objectives is presented. In section 3, simulations are performed on a CarSim™ to verify the effectiveness of updated weighting factor and the performance of the proposed controller, and discussion is made with a comparison of conventional controller for only considering the vehicle lateral stability. Finally, in section 4, conclusions are addressed.

2. DESIGN OF A COOPERATIVE BRAKING CONTROLLER

2.1. Structure of the Proposed Controller

Cooperative regenerative braking controller structure is hierarchical and consists of the direct yaw moment controller based on LQR theory (Upper-level controller) and the brake torque distribution controller (Lower-level controller) using constrained optimization with varying weighting factor. The proposed controller structure is shown in Figure 2. Direct yaw moment controller computes the desired yaw moment based on LQR theory to stabilize the vehicle. The yaw rate and side slip angle from sensors are used to track the desired vehicle motion. Brake torque distribution controller distributes an optimal regenerative brake torque ($T_{regen.}$ in Figure 2) for recovering optimal braking energy and 4 independent mechanical-friction brake torques (T_{FL}, T_{FR}, T_{RL}, T_{RR} in Figure 2) for guaranteeing the vehicle lateral stability. Brake torque distribution controller must guarantee both braking energy recovery performance and the vehicle lateral stability performance including the normal and severe cornering situation. Therefore, for two objectives, brake torque distribution is formulated as constrained optimization which consists of cost function with adaptation of weighting factor, and constraints.

2.2. Design of Direct Yaw Moment Controller based on LQR Theory

In order to improve the vehicle lateral stability, direct yaw moment controller computes the desired yaw moment to track the desired the yaw rate and side slip angle, i.e., to minimize the tracking error. A two degree of freedom linear bicycle model for the vehicle lateral and yaw dynamics is used to design the direct yaw moment con-

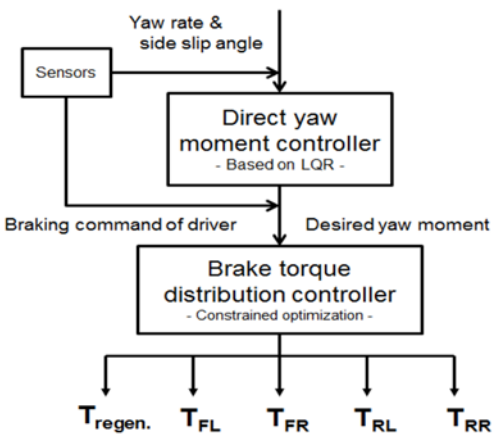

Figure 2. Structure of the proposed controller.

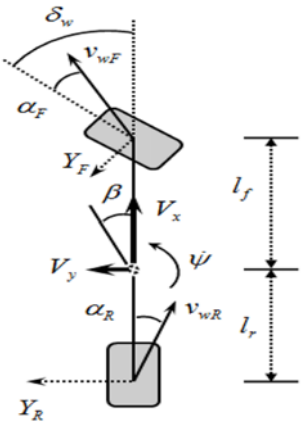

Figure 3. 2 DoF bicycle model for vehicle lateral dynamics.

troller, as shown in figure 3.

Using the body side slip angle and the yaw rate of the vehicle body as state variables, the differential equations of 2-DoF bicycle model can be derived in (1).

$$m \cdot V_x \cdot (\dot{\beta} + \dot{\psi}) = 2(Y_F + Y_R)$$
$$I_z \cdot \ddot{\psi} = 2(l_F \cdot Y_F - l_R \cdot Y_R) + M_{control} \tag{1}$$

Experimental results generally show that the lateral force of a tire is proportional to the slip angle of tire for small slip angle. In Figure 3, the slip angle of a tire is defined as the angle between the orientation of the tire and that of the velocity vector of the wheel. Lateral force of tire is assumed to be linearized for small slip angle as following relation, shown in (2)

$$Y_F = -C_F \cdot \alpha_F, \; Y_R = -C_R \cdot \alpha_R \tag{2}$$

The desired yaw rate and side slip angle tracked is obtained by the driver's steer angle and vehicle speed in (3) and must be bounded by a function of the tire-road friction coefficient in (4) (Rajamani, 2006).

$$\dot{\psi}_{des} = \frac{V_x}{L + mV_x^2(l_R C_R - l_F C_F)/C_R C_F L}\delta_F$$
$$\beta_{des} = \frac{l_R - l_F m V_x^2 / C_R L}{L + mV_x^2(l_R C_R - l_F C_F)/C_R C_F L}\delta_F \tag{3}$$

$$\dot{\psi}_{upper\ bound} = 0.85 \cdot \frac{\mu g}{V_x}, \; \dot{\beta}_{upper\ bound} = \tan^{-1}(0.02\mu g) \tag{4}$$

Tracking error for yaw rate and side slip angle is defined as error between the actual state and the desired state, and error state-space form is derived by using (1), (2), and (3) as follows:

$$\dot{\mathbf{e}} = \dot{\mathbf{x}} - \dot{\mathbf{x}}_{des} = \mathbf{A}\mathbf{e} + \mathbf{B}u + \mathbf{A}\mathbf{x}_{des} + \mathbf{E}r \tag{5}$$

where

$$\mathbf{x} = \begin{Bmatrix} \beta \\ \dot{\psi} \end{Bmatrix}, \; u = M_{control}, \; r = \delta_F, \; A = \begin{bmatrix} a_{11} & a_{12} \\ a_{21} & a_{22} \end{bmatrix},$$
$$B = \begin{bmatrix} b_1 \\ b_2 \end{bmatrix}, \; E = \begin{bmatrix} e_1 \\ e_2 \end{bmatrix}$$

and

$$a_{11} = -\frac{2(C_F + C_R)}{mV_x}, \; a_{12} = -1 - \frac{2(l_F C_F - l_R C_R)}{mV_x^2}$$
$$a_{21} = -\frac{2(l_F C_F - l_R C_R)}{I_z}, \; a_{22} = -\frac{2(l_F^2 C_F + l_R^2 C_R)}{I_z V_x} \tag{7}$$
$$b_1 = 0, \; b_2 = \frac{1}{I_z}, \; e_1 = \frac{2C_F}{mV_x}, \; e_2 = \frac{2l_F C_F}{I_z}$$

Assuming the third and fourth terms are considered as disturbances, LQR theory is applied to minimized the cost function given by (8) (Dincmen and Acarman, 2008; Esmailzadeh *et al*., 2003).

$$J = \int_0^\infty [\mathbf{e}^{\mathbf{T}}\mathbf{Q}\mathbf{e} + u^T \mathbf{R} u]dt \tag{8}$$

where Q and R are the constant weighting matrices.

The solution to optimal control problem that minimizes above cost function is the state feedback gain law in (9) where the optimal gain is obtained by solving the Riccati equation in (10).

$$u = M_{control} = -\mathbf{K_{optimal}} \cdot \mathbf{e} \tag{9}$$

$$\mathbf{A}^{\mathbf{T}}\mathbf{P} + \mathbf{P}\mathbf{A} - \mathbf{P}\mathbf{B}\mathbf{R}^{-1}\mathbf{B}^{\mathbf{T}}\mathbf{P} + \mathbf{Q} = 0,$$
$$\mathbf{K_{optimal}} = \mathbf{R}^{-1}\mathbf{B}^{\mathbf{T}}\mathbf{P} \tag{10}$$

System matrix A can be varied with the vehicle velocity decreased according to driver's braking command. Therefore, optimization process is repeated for vehicle velocity in order to obtain optimal value of feedback gain as function of vehicle velocity (Han *et al*., 2011).

2.3. Design of Brake Torque Distribution Controller

After the control yaw moment is determined by upper-level controller, the brake distribution controller applies two different kinds of brake torques to provide control yaw moments. There are two objectives in this lower-level controller. One is to recover braking energy as much as possible using regenerative braking from electric motor and the other is to keep the vehicle on an intended path as determined by the driver's steer angle input using 4 additional independent mechanical-friction brake torques. However excessive regenerative brake torque in severe cornering can cause the lateral force starts to be decreased, and then the vehicle tends to be under-steer motion. In order to achieve trade-off relationship of two objectives, constrained optimization problem is formulated with newly

defined cost function and several constraints.

2.3.1. Classification of interior region and boundary region of friction circle

The lateral force generation is affected by the presence of braking force. This is the due to the fact that there is limited amount of tire force that can be generated between tire and the road surface. The tire adhesion capability used for generating braking force limits how much lateral force can be generated on tire, and vice versa. This coupled relationship is generally called the "Friction circle" (Pacejka, 2002). By using the concept of friction circle, tire characteristic can be roughly divided two regions. The first region is called as interior region of the friction circle and the second region is called as the boundary region of the friction circle.

Figure 4 shows tire characteristics as the increase of braking force when the vehicle is front steered with constant slip angle. In case 1 where slip ratio of wheel is equal to zero lateral force is only generated by pure lateral slip angle. A further increase of braking force from the case 1 to the case 2 doesn't have great effect on lateral force generation in the first region of tire. This is due to the fact that total force vector sum of lateral force and braking force in case 2 is less than the maximum allowable value of friction force (radius of friction circle: friction coefficient times normal force). In the first region where the effect of braking force on lateral force is relatively small we can neglect the coupled relationship between lateral force and braking force. On the other hand, the further increase of braking force from the case 3 to the case 4 will lead to a reduction in lateral force due to the limited tire adhesion capability. If braking force is increased with constant slip angle, lateral force will be decreased along the boundary of friction circle because that total vector sum of lateral force and braking force in case 3 can't exceed the boundary of friction circle (physical limit of tire). In the second region of tire where the effect of braking force on lateral force is relatively large we must consider the coupled relationship in order to guarantee the vehicle lateral stability.

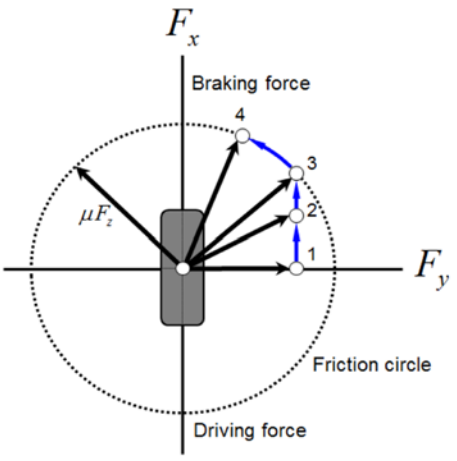

Figure 4. Tire characteristics at constant steer angle.

When the tire comes in interior region of the friction circle, additional control yaw moment for vehicle can be generated by only braking force on each of all wheels assuming that we neglects a small change of lateral force by braking force. Therefore, in this first region of tire, the sum of the braking force on left side wheels and the sum of the braking force on right side wheels are determined from given control yaw moment and required total braking force, as shown in (11).

$$M_{control} = -\frac{t}{2}X_L + \frac{t}{2}X_R$$

$$X_{total} = X_L + X_R \tag{11}$$

$$\Rightarrow \begin{cases} X_L = -\dfrac{M_{control}}{t} + \dfrac{X_{total}}{2} \\ X_R = \dfrac{M_{control}}{t} + \dfrac{X_{total}}{2} \end{cases}$$

And maximum regenerative braking force is equal to the sum of braking force on left side wheels or right wheels, according to the sign of the control yaw moment. For example, if the sign of the control yaw moment is positive, then the maximum regenerative braking force is equal to the sum of the braking force on right side wheels as shown in (12).

$$X_{regn\cdot max} = \max(X_L, X_R) \quad \forall \mathbf{X} < 0 \tag{12}$$

When the tire comes in the boundary region of the friction circle, additional control yaw moment generation for vehicle can be affected by the braking force as well as the change of lateral force by braking force. This is the reason that lateral force would increase/decrease as braking force decreases/increases due to limited tire force. Same amount of braking force on front tires in boundary region of the friction circle can cause more under-steer problem than in interior region of the friction circle. This is due to the fact that decreased lateral force can generate another yaw moment in opposite direction of steering input.

2.3.2. Cost function for including whole regions of friction circle and constraints

The yaw moment distribution for achieving two objectives is formulated as constrained optimization problem. A newly defined cost function must represent trade-off relationship of two objectives and cover the whole regions of tire including interior and boundary region of friction circle. Therefore a weighted sum of the three terms is chosen as the cost function in (13) (Han *et al*., 2011). Moreover, by this cost function, it is possible to adapt weighting factors to recover the maximum regenerative braking energy as well as to guarantee the vehicle lateral stability, even in the severe cornering.

$$\mathbf{x} = \arg\min_{x} f(\mathbf{x}), \quad \forall \mathbf{x} < 0 \tag{13}$$

where

$$f(\mathbf{x}) = a_0[X_{FL} - X_{FR}]^2 + b_0[X_{des} - (X_{FL} + X_{FR})]^2 + c[(\omega_{des} - \omega_{motor})^2 \cdot \max(X_{FL}, X_{FR})^2]$$

With calculated 4 braking forces, regenerative braking force is simply obtained by the regenerative braking characteristic of front-wheel-drive hybrid electric vehicle, as shown in (14)

$$X_{regn.} = \max(X_{FL}, X_{FR}) \tag{14}$$

The objective of first term in cost function is to minimize the difference between braking force on front left wheel and front right wheel. It is possible to symmetrize front braking force. The objective of second term is to minimize the difference between required braking force according to braking command of driver and the sum of the generated braking forces on front wheels. It is possible to increase absolute amount of front braking force rather than rear braking force. The physical meaning of both terms is to maximize regenerative brake torque at front wheels. Moreover the last third term in regard to the motor speed is included in order to determine optimal regenerative braking torque because that regenerative braking power is regenerative brake torque multiplied by motor speed. And the motor speed can be assumed as the speed of front axle with motor inertia because the motor is directly connected to the front axle. Unlike desired motor speed, actual motor speed can be varied according to the value of torque in severe situation on slippery road. Desired motor speed can be obtained by the following relation using gear ratio, vehicle speed and effective radius of tire:

$$\omega_{des} = \zeta \cdot \frac{V_x}{r_{eff}} \tag{15}$$

The physical meaning of third term is to optimize input regenerative braking force in order to recover optimal braking power at every moment.

The tire forces must satisfy the following constraints under the assumption that braking force on front tires is generated by both regenerative brake torque and mechanical-friction brake torques, on the other hand, braking force on rear tires is only generated by mechanical-friction brake torques. The sum of generated braking forces on all four tires by 2 different brake torques should be equal to the required braking force to satisfy driver's braking command with assumption that the value of deceleration from driver can be measured, as shown in (16)

$$X_{FL} + X_{FR} + X_{RL} + X_{RR} = X_{des} \tag{16}$$

where

$$X_{des} = m \cdot a_x$$

Moreover braking force which is generated by brake torques should generate the same amount of the control yaw moment determined from upper-level controller, as shown in (17)

$$\frac{t}{2}(-X_{FL} + X_{FR} - X_{RL} + X_{RR}) = M_{control} \tag{17}$$

2.3.3. Adaptation of weighting factor

As already mentioned, when the vehicle is in normal cornering condition with braking, the lateral force of front tire is within the lateral bound, i.e., in the interior region of friction circle. During normal cornering, constant weighting factor can guarantee the vehicle lateral stability because there is ignorable effect of lateral force on yaw moment generation. On the other hand, when the vehicle is in severe cornering with braking, the braking force limits and even decreases the generation of lateral force on front tire, i.e., in the boundary region of friction circle. This is the reason why that constant weighting factor can cause more under-steer motion for vehicle during severe cornering. Therefore, in order to prevent more under-steer motion by a decrease of the lateral force on front tire, weighting factor must be updated from the state of vehicle lateral motion. third term of cost function in the boundary of the friction circle is more weighted than in other regions because that weighting factor 'c' of third term determines how much regenerative braking force can be decreased for staying within the lateral bounds. Under-steer index is used for representing the state of the vehicle lateral motion, and weighting factor 'c' of third term is newly defined as the function of under-steer index. Conventional under-steer index based on 2 DoF bicycle model is obtained as (18) using lateral acceleration, steer angle input, vehicle speed.

$$K_V = \frac{1}{2}\left[\frac{ml_r}{C_f L} - \frac{ml_f}{C_r L}\right] = \frac{\delta_f}{a_y} - \frac{L}{V_x^2} \tag{18}$$

However, if the lateral acceleration goes to zero, this under-steer index goes to infinity. In order to prevent this problem, new under-steer index is obtained as conventional under-steer index multiplied by lateral acceleration, as shown in (19).

Moreover, weighting factor should be only affected in the boundary region of the friction circle, not in the interior region of the friction circle. It is important to

$$K_V^* = K_V \cdot a_y = \delta_f - \frac{V}{V_x^2} a_y \tag{19}$$

classify two regions of the friction circle. In severe cornering, the driver has to increase the steering angle as slip angle of the front tires is greater than that of rear tires, which is called as under-steer problem. Therefore slip angle of front and rear tires is used to classify two regions.

If slip angle of front tires is greater than that of rear tires, new under-steer index starts to be activated in order to decrease regenerative brake torque by input weighted optimization problem. However, in the vicinity of that front slip angle is almost equal to rear slip angle, under-steer index might be activated even though tire characteristic is not in the boundary of the friction circle. In that case, there is small effect of new under-steer index on weighting factor in cost function because that more braking would result in a decrease of new under-steer index. Pacejka examined the effect of longitudinal forces in cornering with assumption the cornering stiffness may be considered to be dependent on the normal force only. Finally, hyperbolic tangent function is used to prevent chattering problem while crossing the two regions, as shown in (20).

$$K_V^{**} = \frac{1}{2}\left[1+\tanh\left(k_1\left\{\left|\frac{\alpha_{FL}+\alpha_{FR}}{2}\right|-\left|\frac{\alpha_{RL}+\alpha_{RR}}{2}\right|\right\}\right)\right]\cdot K_V^{*} \tag{20}$$

Weighting factor can be obtained as following relationship as in (21).

$$c = c_0\cdot(1+k_2\cdot K_V^{**}) \tag{21}$$

3. SIMULATION

Two kinds of simulations were performed on computer simulation of closed loop driver-vehicle system, CarSim™. The vehicle parameters in the linear model are referred from E-Class SUV in CarSim™ and the basic weighting factor in cost function of proposed controller a_0, b_0, c_0, and the value k_1, k_2 for adaptation of weighting factor 'c' are presented, as given in Table 1.

The first simulation is to analyze the effectiveness of the proposed adaptation method of weighting factor compared to constant weighting factor in severe cornering with constant braking, and second simulation is to analyze the difference between proposed controller and the conventional controller during normal braking scenarios on slippery road. All vehicle performance was evaluated through the vehicle response to a closed loop driver-vehicle system. The steering input is generated by the driver model given in CarSim™. And the tire-road friction coefficient is necessary to design the proposed controller. The tire-road friction coefficient is assumed to be estimated well by real-time friction coefficient estimation algorithm (Ray, 1997; Gustafsson, 1997).

Table 1. Vehicle parameters and the value of basic weighting factor.

m	1862 kg	a_0	1
l_F	1.42 m	b_0	1
l_R	1.53 m	c_0	10^{-4}
C_F	93000 N/rad	k_1	5
C_R	93000 N/rad	k_2	$3*10^4$

3.1. Verification of the Proposed Adaptation Method in Severe Condition

A wet road with tire-road friction coefficient = 0.5 is chosen for simulation, thus, maximum limit of friction force is almost 0.5 g. On circle lane with radius = 152.4 m, the desired lateral acceleration with 100 km/h initial velocity is almost 0.5 g for tracking target road safely. In this section, in order to represent severe cornering situation, a constant brake pedal input has been applied, which is almost 0.2 g. therefore, in this simulation condition, lateral force is limited by the friction limit of the road, and then applied braking force decrease the lateral force.

Figures 5 ~ 8 show the response of SUV vehicle. In figures, solid blue line is for constant 'c' value of cost function which is called as 'w/o adaptation', the dashed red line is for updating 'c' value of cost function for improving more the lateral vehicle stability in even severe cornering which is called as 'w/ adaptation'. As shown figure 5, regenerative brake torque of the vehicle without adaptation of 'c' was more applied than that with adaptation of 'c'. Proposed adaptation method updated the value of 'c' increasingly as the vehicle approached the handling limits in order to decrease the regenerative brake torque. The reason why regenerative brake torque must be decreased by the increase of weighting factor is that yaw moment by the decrease of lateral force corresponding to the increase of regenerative brake torque was generated in opposite direction of steering input and thus the vehicle tended to be more under-steer motion in figure 6. Figure 7 showed that the difference between front slip angle and rear slip angle of 'w/o adaptation' was larger than that of 'w/ adaptation', furthermore, slip angle magnitude of 'w/o adaptation' was also larger than that of 'w/ adaptation'.

Slip angle for front and rear tire was used the average value of the slip angle of left tire and right tire. In other words, the difference of regenerative brake torque between 'w/o adaptation' and 'w/ adaptation' in this simulation condition can make the vehicle be stabilized.

As shown in figure 7, the driver of 'w/o adaptation' required more steer angle than that of 'w/ adaptation' in order to track the target circle trajectory, on the other hand, 'w/ adaptation' by considering the dependency of lateral force and braking force compensated the yaw moment for correcting the vehicle motion and thus can enable the driver to maneuver the vehicle appropriately without steering stress. In figure 8, 'w/ adaptation' made the reachable vehicle trajectory safer compared with 'w/o adaptation'.

Furthermore, 'w/ adaptation' can recover the almost same amount of regenerative braking energy of the case that 'w/o adaptation' applied larger regenerative brake torque than 'w/ adaptation', in table 2. This is due to the fact that 'w/ adaptation' can correct more rapidly the

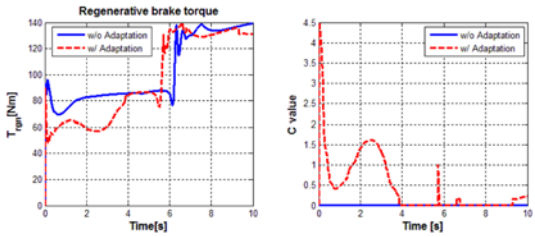

Figure 5. (a) Regenerative brake torque, (b) c value.

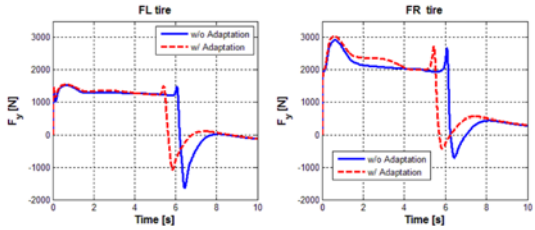

Figure 6. (a) Lateral force of front-left tire, (b) Lateral force of front-right tire.

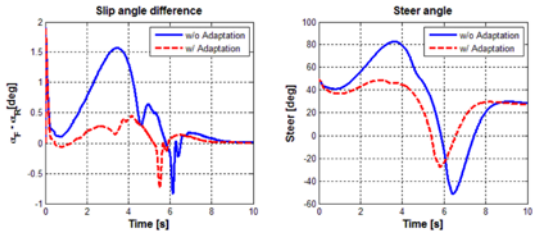

Figure 7. (a) Average slip angle difference between front tire and rear tire, (b) Steer angle.

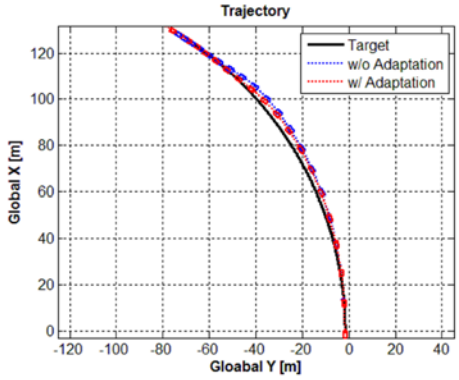

Figure 8. Vehicle trajectory.

vehicle motion than 'w/o adaptation' and 'w/ adaptation' can prevent the large variance in actual motor speed as regenerative brake torque is decreased.

3.2. Comparison with Conventional Controller

From above simulation results, the necessity to update the weighting factor 'c' for guaranteeing the vehicle lateral stability was verified. And the conventional controller is used to compare the performance of recovering the regenerative braking energy as well as that of the vehicle lateral stability with the proposed controller. The conventional controller only focused on guaranteeing the vehicle lateral stability, not recovering the regenerative braking energy. From the concept of friction circle, cost function of the conventional controller is represented for sum of each tire usage. A weighted sum of the absolute normalized forces on the tires is chosen as this cost function, as shown in (22) (Mokhiamar and Abe, 2004; He and Hori, 2006).

Table 2. Regenerative braking energy and braking energy recovery.

Contents	Maximum value	w/o Adaptation	w/ Adaptation
Regenerative braking energy [kJ]	587	323	310
Braking energy recovery [%]	-	55.1	52.9

$$\mathbf{x} = \arg\min_{x} f(\mathbf{x}) \tag{22}$$

where

$$f(\mathbf{x}) = \sum_{i=1}^{4} c_i \cdot \mu_i^2 = \sum_{i=1}^{4} c_i \cdot \frac{X_i^2 + Y_i^2}{Z_i^2}$$

The optimum braking force distribution by this cost function can prevent handling limit of the vehicle. If the sum of resultant tire force which is vector sum of lateral force and braking force on each tire is minimized at any situations, all 4 resultant tire forces must exist within the physical limit of adhesion of the tire and are finally utilized the maximum tire force possible. On the other hand, this cost function can't increase regenerative braking force on front tires up to the maximum allowable value of tire force due to that this cost function must distribute the braking forces on rear tires.

Final braking section of Europe Urban Driving Cycle (EUDC, in the figure 9) [347s – 377s] is chosen to describe normal braking scenario of driver in city. The normal braking scenario is divided by two parts as follows: First and second part are chosen as required braking deceleration of driver from 347s to 362s, and from 363s to 377s in EUDC, respectively. The key objective of all simulation results is to analyze how much braking energy recovery of proposed controller can be improved while vehicle lateral stability must be guaranteed, in comparison with the conventional controller. All figures show the response of SUV vehicle on Carsim™. In figures, solid blue line is for only regenerative braking on front tire which is called as 'w/o control', the dashed red line is for conventional controller, and the dash dotted cyan line is for proposed controller.

In order to investigate the effect of the proposed con-

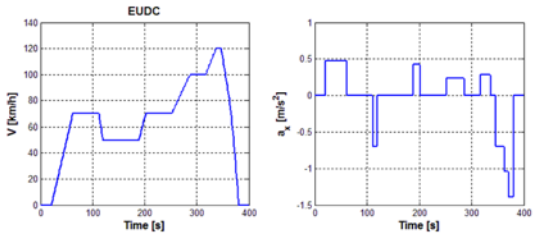

Figure 9. Velocity and deceleration of EUDC.

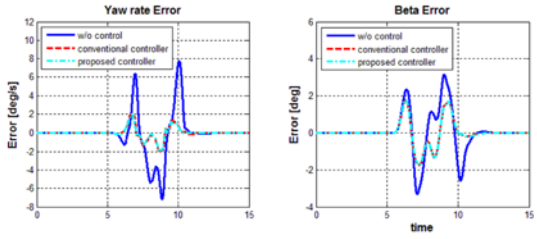

Figure 10. First part of EUDC: Yaw rate error & Side slip angle (Beta) error.

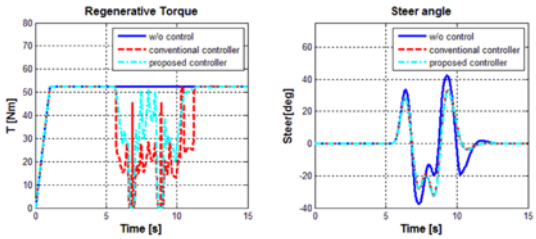

Figure 11. First part of EUDC: Regenerative brake torque & Steer angle by driver model.

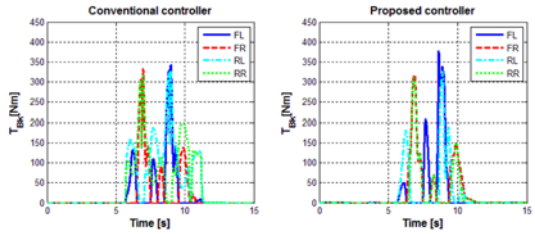

Figure 12. First part of EUDC: Mechanical-friction brake torque distribution of each controller.

troller on braking energy recovery performance when the vehicle must avoid an obstacle in an emergency situation, simulation subjected to evasive double lane change was performed on a wet road, which means maximum tire fricition force is almost 0.5 g. Figures 10 ~ 13 show the results of first part of normal braking scenario in EUDC.

As shown in figure 10, the yaw rate errors and side-slip angle errors for the conventional controller and the proposed controller were almost same during evasive double lane change situation. Figure 11 shows the applied regenerative

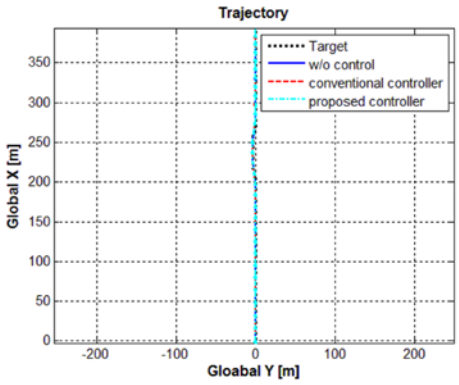

Figure 13. Vehicle trajectory.

brake torque and steer angle for each controller and figure 12 shows the applied mechanical-friction brake torques for each controller. In figure 12, the legends FL, FR, RL, and RR represent the front left, front right, rear left, rear right wheel, respectively. Both controllers apply additional mechanical-friction brake torques to generate control yaw moment in order to track the intended path. The distribution of between the regenerative brake torque and mechanical-friction brake torques for proposed controller was different from conventional controller despite of same control yaw moment determined from upper-level controller, in figures 11 ~ 12. As shown in figure 12, the conventional controller tended to distribute evenly braking force for each tire in order to minimize the sum of all tire usage, even in the situation where increasing regenerative braking force didn't affect the lateral force on front tire. On the other hand, the proposed controller prioritized regenerative braking on front tire first until its frictional limit where it is no longer possible to keep the lateral force. Furthermore adaptation method in the proposed controller must decrease the regenerative brake torque at front wheels in only situation where under-steer motion of vehicle was happened. As shown in figure 13, all vehicles can be driven safely during evasive double lane change.

As shown figures 9 ~ 10, uncontrolled vehicle generated large yaw rate error and side-slip angle error, and the driver must generate large steer angle in order to maneuver the vehicle correctly, compared with all controlled vehicles.

In order to investigate the effect of the proposed controller on braking energy recovery performance when the vehicle is operated near the limits of adhesion, simulation subjected to constant turning was performed on an icy road. Maximum friction force on icy road and the desired lateral acceleration with initial velocity of second part of nomal braking scenario are same as 0.3 g.

Figures 14 ~ 17 show the results of second part of normal braking scenario in EUDC. Vehicle response to constant turning resulted in unstable vehicle motion in case of uncontrolled vehicle. Regenerative braking force on front tires of uncontrolled vehicle decreased the lateral forces due to nonlinear characteristic of tire. This effect

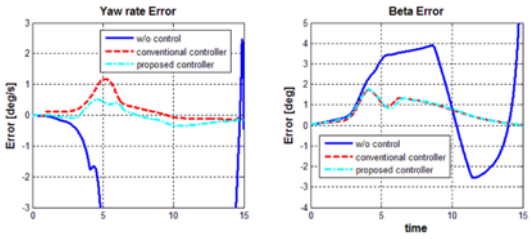

Figure 14. Second part of EUDC: Yaw rate error & Side slip angle (Beta) error.

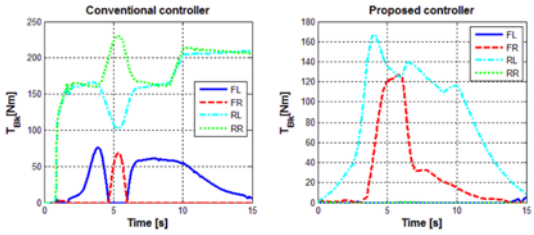

Figure 16. Second part of EUDC: Mechanical-friction brake torque distribution of each controller.

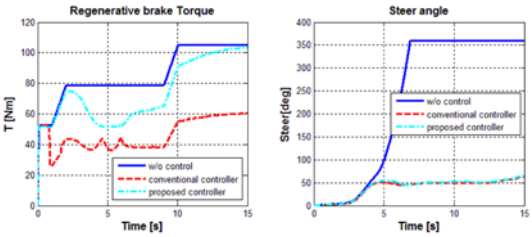

Figure 15. Second part of EUDC: Regenerative brake torque & Steer angle by driver model.

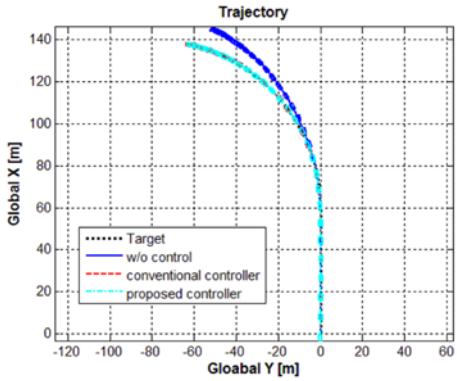

Figure 17. Second part of EUDC: Vehicle trajectory.

resulted in the loss in steer-ability for driver in figure 15. Unlike the results of evasive double lane change, those of constant turning show a definite difference of brake torque distribution trends between the proposed controller and the conventional controller. This was due to the fact that continuous lateral acceleration in positive direction increased the normal force on right-side tires, whereas it decreased the normal force on left-side tires.

Conventional controller applied more braking force on right-side tires than on left-side tires. As shown in figure 15, it resulted in decreasing more the symmetric regenerative brake torque, whereas increasing more mechanical-friction brake torque at rear-right wheel, in comparison with the proposed controller. Figure 17 show vehicle with controllers stabilized the vehicle motion compared to uncontrolled vehicle.

Table 3 shows the regenerative braking energy and the braking energy recovery. As shown in table 3, available maximum braking energy during first and second normal braking scenario, which can be recovered through regenerative braking, is 664KJ and 352KJ, respectively. Braking energy recovery was obtained by a ratio of regenerative braking energy over the maximum braking energy. In comparison with the conventional controller, the proposed controller improved 6.2% during first part of scenario and 27.4% during second part of scenario in terms of braking energy recovery performance.

In order to verify the improved braking energy recovery performance of the proposed controller in comparison with the conventional controller, simulations performed in different scenarios with several driving cycles such as Japan 11 mode, the New York City Cycle (NYCC), USA CITY 1, etc. As shown in figure 18, first, second and third normal braking scenario are chosen as required braking deceleration from 67s to 77s in Japan 11 mode, from 232s to 240s in NYCC, from 300s to 325s in USA CITY 1. In figure 19, the icy road is the reference trajectory for first, second normal braking scenario and the wet road is the reference trajectory for third normal braking scenario. Maximum friction force on the icy road is almost 0.3 g and that on the wet road is almost 0.5 g.

The proposed controller and the conventional controller

Table 3. Regenerative braking energy and braking energy recovery of controllers.

	Contents	Maximum value	Proposed controller	Conventional controller
First part of EUDC [347s - 362s]	Regenerative braking energy [kJ]	664	412	371
	Braking energy recovery [%]	-	62.0	55.8
Second part of EUDC [363s - 377s]	Regenerative braking energy [kJ]	352	276	180
	Braking energy recovery [%]	-	78.4	51.0

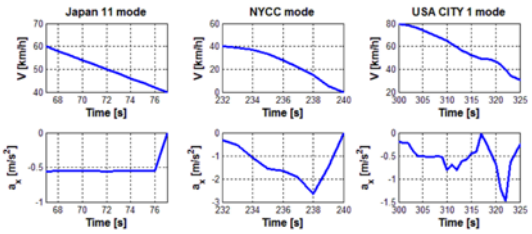

Figure 18. Velocity and deceleration in several driving cycle.

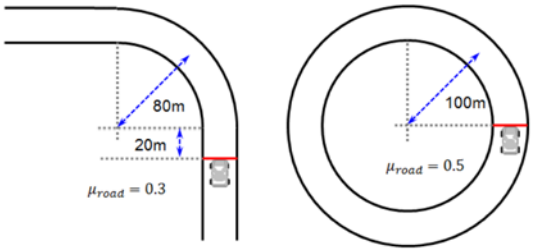

Figure 19. 1: Icy road, 2: wet road.

for three scenarios show the similar performance of the vehicle lateral stability. When the vehicle tended to be under-steer motion, all controllers engaged and then distributed regenerative brake torque as well as mechanical-friction brake torques to generate the control yaw moment in order to keep the vehicle on an intended path, assisting the driver to effectively generate the steer angle. Table 4 shows regenerative braking energy and braking energy recovery for three scenarios. In comparison with the conventional controller, the proposed controller improved 24.5% at 62s-77s in Japan 11 mode, 30.2% at 232s-240s in NYCC mode and 15.6% at 300s-325s in USA CITY 1 mode in terms of braking energy recovery performance.

4. CONCLUSION

In this paper, a design method of cooperative regenerative braking controller was proposed to maximize the braking energy recovery while guaranteeing the vehicle lateral stability. In order to generalize the constrained optimization problem including the normal and severe cornering situations, adaptation method of weighting factor was also proposed. Severe cornering simulation results showed the effectiveness of weighting factor adaptation on the vehicle handling performance. If weighting factor is updated to increase as front tires lose friction with surface of the road, the vehicle with adaptation method achieved higher lateral vehicle stability than the vehicle without adaptation method. In conclusion, increased corrective yaw moment generated by braking forces on the rear tires resulted in increasing the vehicle lateral stability within the physical limit of adhesion of the tires.

From the simulation results of severe scenarios which describes realistic braking situation for normal driver in city, it is concluded that the vehicle with the proposed controller became stable for the normal driver similar to the conventional controller. All simulation results were compared with the conventional controller which only focused on the usage of tire usage for the vehicle lateral stability. In terms of the performance of braking energy recovery the proposed controller improved definitely in all scenarios in comparison with the conventional controller. Future work will evaluate the performance of the proposed controller through experiment test.

ACKNOWLEDGEMENT–This work was supported by the National Research Foundation of Korea (NRF) grant funded by the Korea government (MEST) (No. 2010-0028680), and the BK21 program.

REFERENCES

Chu, L., Sun, W., Yao, L. and Zhang, Y. (2009). Integrative control strategy for regenerative and hydraulic braking for hybrid electric car. *Proc. IEEE Veh. Power Propuls. Conf. 2009*, 1091–1098.

Dincmen, E. and Acarman, T. (2008). Active coordination of the individually actuated wheel braking and steering to enhance vehicle lateral stability and handling. *Proc. The 17th World Cong. 2008*, 10738–10743.

Esmailzadeh, E., Goodarzi, A. and Vossoughi, G. R. (2003). Optimal yaw moment control law for improved vehicle handling. *Mechatronics* **13**, **7**, 659–675.

Gao, Y., Chu, L. and Ehsani, M. (2007). Design and control

Table 4. Regenerative braking energy and braking energy recovery in several braking scenario.

	Contents	Maximum value	Proposed controller	Conventional controller
JAPAN 11 Mode [67s - 77s]	Regenerative braking energy [kJ]	152	98.3	61.0
	Braking energy recovery [%]	-	64.5	40.0
NYCC Mode [232s - 240s]	Regenerative braking energy [kJ]	117	99.3	64.2
	Braking energy recovery [%]	-	85.2	55.0
USA CITY 1 Mode [300s - 325s]	Regenerative braking energy [kJ]	411	217	153
	Braking energy recovery [%]	-	52.7	37.1

principle of hybrid braking system for EV, HEV and FCV. *Proc. IEEE Veh. Power Propuls. Conf. 2007*, 384–391.

Gustafsson, F. (1997). Slip-based tire-road friction estimation. *Automatica* **33**, **6**, 1087–1099.

Han, J. and Park, Y. (2011). Cooperative regenerative braking control strategy considering nonlinear tire characteristic in front-wheel-drive hybrid electric vehicle. *SAE Paper No.* 2011-39-7209.

Han, J., Park, Y. and Park, Y. (2011). Adaptive regenerative braking control in severe cornering for guaranteeing the vehicle stability of fuel cell hybrid electric vehicle. *Proc. IEEE Veh. Power Propuls. Conf. 2011*, 1–5.

Hancock, M. and Assadian, F. (2006). Impact of regenerative braking on vehicle stability. *Proc. IET Hybrid Veh. Conf. 2006*, 173–184.

He, P. and Hori, Y. (2006). Improvement of EV maneuverability and safety by disturbance observer based dynamic force distribution. *Proc. EVS22*, 1818–1827.

Hellgren, J. and Jonasson, E. (2007). Maximisation of brake energy regeneration in a hybrid electric parallel car. *Int. J. Electric and Hybrid Vehicles* **1**, **1**, 95–121.

Hori, Y. (2004). Future vehicle driven by electricity and control–Research on four-wheel-motored "UOT electric march II". *IEEE Trans. Ind. Electron.* **51**, **5**, 954–962

Jingming, Z., Baoyu, S. and Xiaojing, N. (2008). Optimization of parallel regenerative braking control strategy. *Proc. IEEE Veh. Power Propuls. Conf. 2008*, 1–4.

Kim, D. and Kim, H. (2006). Vehicle stability control with regenerative braking and electronic brake force distribution for a four-wheel drive hybrid electric vehicle. *Proc. Inst. Mech. Eng., Part D: J. Automobile Eng.* **220**, **6**, 683–693.

Kim, D., Kim, J., Hwang, S. and Kim, H. (2007). Optimal brake torque distribution for a four-wheel-drive hybrid electric vehicle stability enhancement. *Proc. Inst. Mech. Eng., Part D: J. Automobile Eng.* **221**, **11**, 1357–1366.

Mokhiamar, O. and Abe, M. (2004). Simultaneous optimal distribution of lateral and longitudinal tire forces for the model following control. *J. Dyn. Syst. Meas. Control* **126**, **4**, 753–763.

Mutoh, N., Hayano, Y., Yahagi, H. and Takita, K. (2007). Electric braking control methods for electric vehicles with independently driven front and rear wheels. *IEEE Trans. Ind. Electron.* **54**, **2**, 1168–1176.

Oleksowicz, S. A., Burnham, K. J., Barber, P., Toth-Antal, B., Waite, G., Hardwick, G., Harrington, C. and Chapman, J. (2013). Investigation of regenerative and anti-lock braking interaction. *Int. J. Automotive Technology* **14**, **4**, 641–650.

Pacejka, H. B. (2002). *Tire and Vehicle Dynamics*. Society of Automotive Engineers and Butterworth-Heinemann. Oxford.

Rajamani, R. (2006). *Vehicle Dynamics and Control*. Springer. New York.

Ray, L. R. (1997). Nonlinear tire force estimation and road friction identification: Simulation and experiment. *Automatica* **33**, **10**, 1819–1833.

Sakai, S., Sado, H. and Hori, Y. (1999). Motion control in an electric vehicle with four independently driven in-wheel motors. *IEEE/ASME Trans. Mechatron* **4**, **1**, 9–16.

Shino, M. and Nagai, M. (2003). Independent wheel torque control of small-scale electric vehicle for handling and stability improvement. *JSAE Review* **24**, **4**, 449–456.

Wang, X., Shi, S., Liu, L. and Jin, L. (2013). Analysis of driving mode effect on vehicle stability. *Int. J. Automotive Technology* **14**, **3**, 363–373.